Hole pairing and phonon dynamics in generalized two-dimensional t-J Holstein models

T. Sakai
Laboratoire de Physique Quantique, Université Paul Sabatier, 31062 Toulouse, France
and Faculty of Science, Himeji Institute of Technology, Kanaji, Kamigori, Ako-gun, Hyogo 678-12, Japan

D. Poilblanc
Laboratoire de Physique Quantique, Université Paul Sabatier, 31062 Toulouse, France

D. J. Scalapino
Department of Physics, University of California, Santa Barbara, California 93106
(Received 13 September 1996; revised manuscript received 10 December 1996)

The formation of hole pairs in the planar t-J model is studied in the presence of independent *dynamic* vibrations of the in-plane oxygen atoms. In-plane (breathing modes) and out-of-plane (buckling modes) displacements are considered. We find strong evidence in favor of a stabilization of the two-hole bound pair by out-of-plane vibrations of the in-plane oxygens. On the contrary, the breathing modes weaken the binding energy of the hole pair. When properly dressed by oxygen buckling fluctuations, the hole-pair propagator exhibits a large quasiparticlelike peak. These results are discussed in the context of superconducting cuprates. [S0163-1829(97)00313-5]

I. INTRODUCTION

The electron-phonon interaction plays the key role in the conventional BCS theory of superconductivity. It is the source of the effective (retarded) attraction between the electrons and hence of the dynamical effect for pair formation. On the contrary, in unconventional superconductors like the high-T_c cuprates, the driving force for superconductivity is commonly believed to be the strong electronic correlations. However, it is theoretically known that, in strongly correlated systems, even moderate electron-phonon interactions can have drastic consequences. For example, it can enhance charge-density-wave and spin-density-wave instabilities due to polaronic self-localization effect.[1,2] Experimentally, the observation of some oxygen isotope effect in the high-T_c cuprates[3] has given evidence for some contribution of the electron-phonon interaction in the superconductivity, even though the dominant pairing mechanism is due to strong antiferromagnetic correlations. The interplay between strong electronic correlations and electron-phonon interaction still remains an open question.

For the sake of simplicity, we describe here the low-energy electronic degrees of freedom by a single band t-J model. We also restrict ourselves to the vibrations of the in-plane oxygen atoms of the CuO_2 plane which have been shown to be essential. Two types of displacement have to be considered: (a) in-plane breathing modes and (b) buckling modes, as shown schematically in Fig. 1. When the equilibrium position of the oxygen atom lies away from the Cu plane by u_0 in Fig. 1(b), the electron-phonon interaction becomes linear in the oxygen displacement perpendicular to the plane,[4] as it is always the case for the breathing modes. Such a buckling structure is realized in $YBa_2Cu_3O_{7-\delta}$. In the antiadiabatic limit the two modes of interaction give an effective nearest-neighbor (NN) hole-hole repulsion (a) and attraction (b), respectively. Using a Hartree-Fock mapping with a tight-binding dispersion, Song and Annett[5] found that the breathing mode suppresses d-wave superconductivity. In a weak-coupling t-matrix approximation which included a random-phase approximation antiferromagnon spin-fluctuation exchange and a phonon exchange, Bulut and Scalapino[6] found that the buckling mode can enhance $d_{x^2-y^2}$ pairing. Using an antiferromagnetic-induced hole dispersion and treating the electron-phonon interaction at the mean-field level, Nazarenko and Dagotto[7] found that the buckling mode can give rise to a $d_{x^2-y^2}$ wave superconducting ground state (GS). However, both of these results involve uncontrolled approximations which are inadequate for treating the Hubbard and t-J models in the absence of phonons. In addition, retardation effects in the phonon-mediated electron-electron interaction might play a very crucial role. Thus it is of interest to carry out a numerical investigation of this problem. Our results are based on exact diagonalization studies of small t-J-phonon clusters. In agreement with the

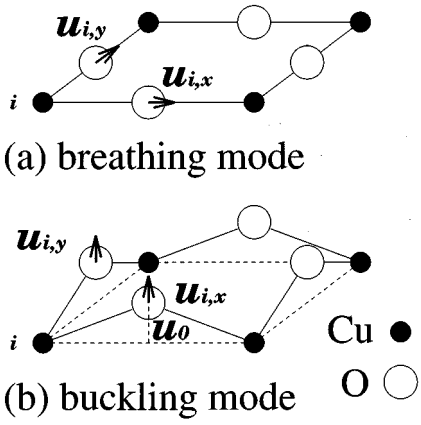

FIG. 1. Schematic lattice displacements of breathing (a) and buckling (b) modes in the CuO_2 plane.

approximate results we find that the breathing mode suppresses the two-hole pairing,[6] while the buckling mode stabilizes it.[6,7] However, in addition, we have examined the effect of the phonons on the kinetic energy, antiferromagnetic structure factor, and hole-hole correlations, giving a more detailed picture of the role of dynamic lattice vibrations on the hole pairing.

II. MODELS AND METHODS

The Hamiltonian is a generalization of the t-J Holstein Hamiltonian[8],

$$H=-t\sum_{\langle \mathbf{i},\mathbf{j}\rangle,\sigma}(\tilde{c}^{\dagger}_{\mathbf{j},\sigma}\tilde{c}_{\mathbf{i},\sigma}+\tilde{c}^{\dagger}_{\mathbf{i},\sigma}\tilde{c}_{\mathbf{j},\sigma})+J\sum_{\langle \mathbf{i},\mathbf{j}\rangle}\left(\mathbf{S}_{\mathbf{i}}\cdot\mathbf{S}_{\mathbf{j}}-\frac{1}{4}n_{\mathbf{i}}n_{\mathbf{j}}\right)+\sum_{\mathbf{i},\boldsymbol{\delta}}\left(\frac{p^2_{\mathbf{i},\delta}}{2m}+\frac{1}{2}m\Omega^2u^2_{\mathbf{i},\delta}\right)+g\sum_{\mathbf{i},\delta}u_{\mathbf{i},\delta}(n^h_{\mathbf{i}}\mp n^h_{\mathbf{i}+\delta}), \quad (1)$$

where $\tilde{c}^{\dagger}_{\mathbf{i},\sigma}$ is the usual hole creation operator, $n_{\mathbf{i}}$ and $n^h_{\mathbf{i}}$ are the electron and hole local densities respectively, m is the oxygen ion mass, Ω is the phonon frequency, and $\delta=\mathbf{x},\mathbf{y}$ differentiates the bonds along the x and y direction, respectively. The sign $-$ $(+)$ in the last term corresponds to the breathing (buckling) mode. Throughout, energies are measured in unit of the hopping integral t. The electron-phonon g term involves the coupling of each copper hole with the displacements of the four neighboring oxygens $u_{\mathbf{i},\delta}$ and $u_{\mathbf{i}-\delta,\delta}$. This is clearly different from the on-site Holstein coupling[9] which has been recently used to mimic the coupling with the apical oxygen modes in the framework of the t-J model.[10] Note that the displacements $u_{\mathbf{i},\delta}$ are considered throughout as *independent* variables. For the purpose of our discussion it is convenient to rewrite the electron-phonon interaction in the boson representation of the phonons,

$$H_{\text{e-ph}}=\Omega\sum_{\mathbf{i},\delta}\left(b^{\dagger}_{\mathbf{i},\delta}b_{\mathbf{i},\delta}+\frac{1}{2}\right)+\lambda_0\sum_{\mathbf{i},\delta}(b_{\mathbf{i},\delta}+b^{\dagger}_{\mathbf{i},\delta})(n^h_{\mathbf{i}}\mp n^h_{\mathbf{i}+\delta}), \quad (2)$$

where $\lambda_0=g\sqrt{1/2m\Omega}$. Since the phononic Hilbert space has an infinite dimension, we truncate it to a finite number of bosonic states, i.e., $b^{\dagger}_{\mathbf{i},\delta}b_{\mathbf{i},\delta}\leqslant n_{\text{ph}}$ at each oxygen site. We restrict ourselves to $n_{\text{ph}}=1$. To test the validity of the one-phonon approximation, the one-hole GS energy of the 2×2 cluster for $J=0.3$ and $\Omega=0.2$ is plotted versus lattice with n_{ph} up to 5 for the breathing and buckling modes, in Figs. 2 (a) and 2(b) respectively. The polaronic effect is revealed to be larger for the buckling mode. However, for both modes, the converging behavior for $n_{\text{ph}}\geqslant2$ suggests that the one-phonon calculation is a good approximation in the weak-coupling region ($\lambda\leqslant0.3$). We have also checked[11] that the behaviors with the coupling constant λ_0 of the various relevant physical quantities are found to be unsensitive to n_{ph} in the region, although $n_{\text{ph}}=1$ generally *underestimates* the role of the phonons. This truncation procedure enables us to study a $\sqrt{8}\times\sqrt{8}$ unit-cell cluster with all the phonon modes (16 modes). We investigate the one- and two-hole GS of Hamiltonian (1) in a regime ($0.3\leqslant J\leqslant0.5$) where, in the absence of phonons, the two-hole pairing state is stabilized by the antiferromagnetic correlation, and we take a realistic

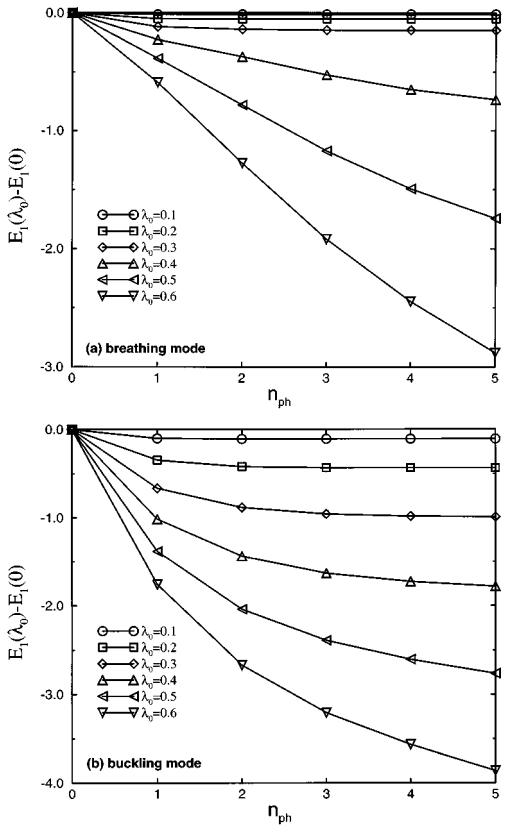

FIG. 2. One-hole ground state energy vs truncated phonon number n_{ph} at each oxygen site on the 2×2 cluster (i.e., Cu_4O_8) with breathing (a) and buckling (b) modes.

phonon frequency $\Omega=0.2$. Since the $\sqrt{8}\times\sqrt{8}$ cluster with periodic boundary conditions has the C_{4v} symmetry, we concentrate on the lowest state with the $d_{x^2-y^2}$ symmetry as the two-hole GS. Although this state is not the GS for small J ($J<0.43$) and $\lambda_0=0$ due to finite-size effects, this choice is justified by the fact that the two-hole GS has $d_{x^2-y^2}$ symmetry in the thermodynamic limit.

III. SELF-LOCALIZATION EFFECT

At first we consider the polaronic self-localization effect on a single hole motion. In general the lattice distortions make the effective mass of the hole larger and the effect can lead to self-localization of the hole. The breathing lattice deformations around the hole lower the potential at the hole site, while they raise that at the nearest-neighbor Cu sites. On the contrary, the buckling deformations lower that at the nearest-neighbor Cu sites as well as at the hole site. Thus the mass renormalization due to the buckling mode is expected to be smaller in the antiadiabatic limit. The kinetic energy *per hole* in the GS of a system with N_h holes,

$$E_{\text{kin}}=\left\langle -t\sum_{\langle \mathbf{i},\mathbf{j}\rangle,\sigma}(\tilde{c}^{\dagger}_{\mathbf{j},\sigma}\tilde{c}_{\mathbf{i},\sigma}+\tilde{c}^{\dagger}_{\mathbf{i},\sigma}\tilde{c}_{\mathbf{j},\sigma})\right\rangle \Big/ N_h \quad (3)$$

is shown as a function of λ_0 in Fig. 3. For the one-hole GS, the absolute value $|E_{\text{kin}}|$ decreases significantly with increasing λ_0 for the breathing mode, while it does not change significantly for the buckling mode. This is a sign that

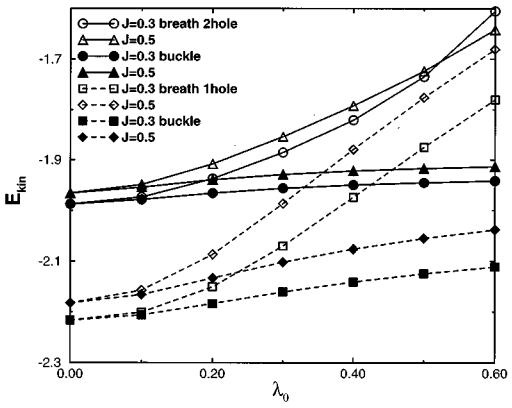

FIG. 3. Kinetic energy $E_{\rm kin}$ per hole in the Cu_8O_{16} cluster for $\Omega=0.2$. Open (solid) symbols correspond to the breathing (buckling) mode. Solid (dashed) lines refer to the two (one) hole GS.

only the breathing mode leads to a polaronic self-trapping process. The difference between the two modes is also clear from the behavior of the spin structure factor in the one-hole GS

$$S_s(\pi,\pi)=\left\langle\left(\sum_{\mathbf{i}}(-1)^{(i_x+i_y)}S^z_{\mathbf{i}}\right)^2\right\rangle \tag{4}$$

shown in Fig. 4. A significant increase of $S_s(\pi,\pi)$ occurs around $\lambda_0=0.1$ almost independently of J for the breathing mode. The agreement between the behaviors of $S_s(\pi,\pi)$ and $E_{\rm kin}$ vs λ_0 suggests that the increase of the effective mass of the hole due to a polaronic self-localization effect leads, for the breathing mode, to an enhancement of the antiferromagnetic spin correlation. Figure 4 also shows that the buckling mode, on the contrary, does not lead to any crossover characteristic of self-localization.

IV. HOLE PAIRING

The two-hole binding energy is a good probe to test the formation of pair of holes. It is defined as

$$\Delta_2=E_0^{(2)}+E_0^{(0)}-2E_0^{(1)}, \tag{5}$$

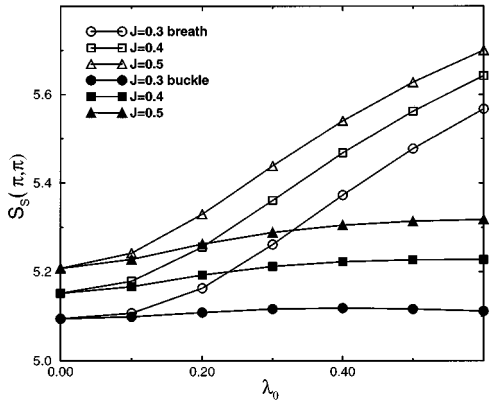

FIG. 4. Spin structure factor $S_s(\pi,\pi)$ of Cu_8O_{16} for a single hole and $\Omega=0.2$. Open (solid) symbols correspond to the breathing (buckling) mode.

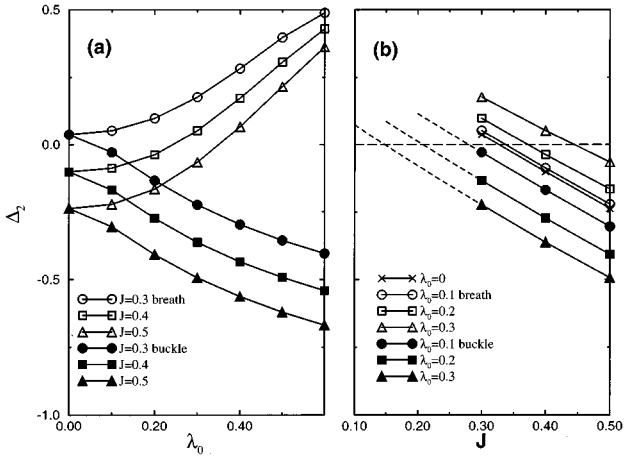

FIG. 5. Two-hole binding energy Δ_2 calculated on Cu_8O_{16} for $\Omega=0.2$ (a) plotted vs λ_0 for fixed J, (b) plotted vs J for fixed λ. Open (solid) symbols correspond to the breathing (buckling) mode.

where $E_0^{(p)}$ is the GS energy for a system with $N_h\equiv\Sigma_{\mathbf{i}}n^h_{\mathbf{i}}=p$. $E_0^{(0)}$ corresponds to the energy of the antiferromagnetic background. A negative value of Δ_2 indicates the stability of a two-hole bound state, as was established for the pure t-J model.[12,13] Figure 5(a), where Δ_2 is displayed as a function of λ_0, clearly shows that the buckling mode stabilizes the two-hole bound state while the breathing mode suppresses it. The effect of the electron-phonon interaction is to shift the boundary of the pairing phase of the t-J model: the buckling mode enlarges the phase toward small J while the breathing mode reduces it, as revealed in Fig. 5(b). The behavior of Δ_2 suggests the possibility that the buckling mode assists superconductivity in the high-T_c cuprates, while the breathing mode suppresses it. We note that, for the buckling mode, no self-trapping process occurs even in the two-hole state, since there is no significant decrease of the kinetic energy in Fig. 3. Thus the hole pair is not localized and can contribute to superconductivity.

The previous data suggest that the electron-phonon interaction acts as an effective attraction (repulsion) between holes for the buckling (breathing) mode, apparently in agreement with the antiadiabatic limit. However, for a finite phonon frequency, it is not clear, *a priori*, whether the phonon-mediated interaction can be reduced to a static potential. To test this possibility, we consider the expectation value of the hole-hole distance in the two-hole GS

$$d_h=\left\langle\sum_{\mathbf{i}\neq\mathbf{j}}n^h_{\mathbf{i}}n^h_{\mathbf{j}}|\mathbf{j}-\mathbf{i}|\right\rangle\Big/\left\langle\sum_{\mathbf{i}\neq\mathbf{j}}n^h_{\mathbf{i}}n^h_{\mathbf{j}}\right\rangle. \tag{6}$$

Figure 6 shows that, for the breathing mode, d_h increases almost monotonously with increasing λ_0 in agreement with the effective NN hole-hole repulsion derived in the antiadiabatic limit. However, d_h for the buckling mode does not show the behavior expected for a NN static attraction. On the contrary, it would rather correspond to a small NN static repulsion, at least for small $\lambda_0(<0.2)$. In any case, the change of d_h with the electron-phonon coupling constant is much too small to explain by itself the effective attraction between the two holes.[14] Clearly, a dynamical interaction is needed. The failure of the antiadiabatic picture, in this case,

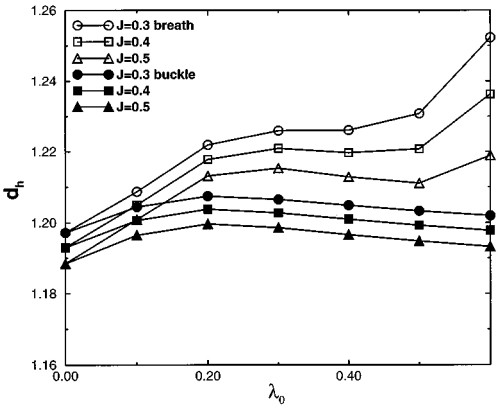

FIG. 6. Hole-hole distance in the two hole GS for $\Omega=0.2$. Open (solid) symbols correspond to the breathing (buckling) mode.

suggests that the effective hole-hole interaction stabilizing the hole pairing is controlled by an essentially dynamical effect of the electron-phonon interaction and some retardation makes the range of the effective hole-hole attraction longer. In other words, the stabilization of the hole binding cannot be understood simply in terms of a static NN attraction but rather involves more subtle retardation effects.

Some of the dynamical effects of the electron-phonon interaction can be estimated from the lattice deformation (per hole) around the hole sites

$$D_h=-\left\langle \sum_{\mathbf{i},\delta} (b_{\mathbf{i},\delta}+b^{\dagger}_{\mathbf{i},\delta})(n^h_{\mathbf{i}}\mp n^h_{\mathbf{i}+\delta})\right\rangle \Big/ N_h, \qquad (7)$$

where $-$ $(+)$ corresponds to the breathing (buckling) mode. It is proportional to the absolute value of the energy of the electron-phonon interaction. D_h is always positive, which means that the oxygen ion deformation toward the neighboring hole sites is favored. D_h is essentially a dynamical quantity which should be distinguished from the total lattice deformaton $D_{\rm tot}$ given by replacing $(n^h_{\mathbf{i}}\mp n^h_{\mathbf{i}+\delta})/N_h$ by unity in the form (7). The static quantity $D_{\rm tot}$ is always zero except when $\Omega=0$. Figure 7 shows that, for the buckling mode, the deformation per hole D_h in the two-hole state is larger than the one in the single hole state, in contrast to the case of the breathing mode. Thus, with buckling modes, the pair takes advantage of a larger deformation around the holes. On the contrary, the breathing deformations lead to an energy loss in the pairing state. Thus, the relative change of the lattice contraction around the holes in the paired state ultimately contributes to a decrease or an increase of the binding energy. Particularly for the buckling mode, the energy gain coming from the lattice deformation clearly dominates the behavior of the binding energy, since no significant change appears in the kinetic energy (Fig. 3) or in the antiferromagnetic correlation which can be estimated from the spin structure factor $S_s(\pi,\pi)$ in Fig. 4. In other words, buckling modes stabilize the hole pairing state dynamically, with little changes in the static features.

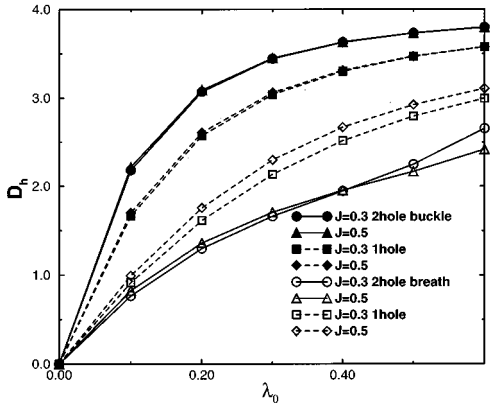

FIG. 7. Lattice deformation (per hole) around the hole sites for $\Omega=0.2$. Open (solid) symbols correspond to the breathing (buckling) mode. Solid (dashed) lines refer to the two (one) hole GS.

This is to be contrasted to the case of the breathing mode which can modify some static properties. As λ_0 increases, the effective mass becomes larger due to the polaronic self-trapping process and, as a result, the antiferomagnetic correlation increases. Since the self-localization effect in the two-hole state is smaller than the one-hole state (Fig. 3), this effect might tend to stabilize some trapped two-hole bound states. However, a larger effective repulsion due to the dynamical lattice deformation overcomes the static effect and suppresses the hole pairing in the presence of breathing modes.

V. DYNAMICAL CORRELATION FUNCTIONS

In this section we propose phonon-dressed operators describing hole-polaron and bi-polaron states and discuss the dynamical correlation function associated with these operators. Particularly the dynamical pair spectral function highlights the dynamical features of the phonon-mediated interaction. We concentrate on the buckling vibrations because they stabilize the hole pairing.

A. Single polaron

First, we shall consider a single-polaron operator describing the one-hole state with a momentum k. Since the size of the polaron (which can easily be estimated) is small, phonons at the nearest oxygen sites of the hole play the most important role and, hence, we only take them into account. We restrict ourselves only to up to one phonon at every oxygen site adjacent to the hole site. Thus, in our framework, up to four phonons could be included. This second restriction is justified by the fact that, in the small coupling region, the average number of excited phonons per site is much smaller than one. The quasiparticle operator should have the same symmetry as the one-hole ground state. Under these conditions a general form of a composite polaron operator with momentum k is

$$\overline{c_{\mathbf{k},\sigma}}=\sum_{\mathbf{i}} e^{i\mathbf{k}\cdot\mathbf{i}}\tilde{c}^{\dagger}_{\mathbf{i},\sigma}\Big[\gamma^{(0)}+\sum_{\alpha}\gamma^{(1)}_{\alpha}\hat{\phi}^{(1)}_{\alpha} +\sum_{\alpha}\gamma^{(2)}_{\alpha}\hat{\phi}^{(2)}_{\alpha}+\cdots\Big]_{\mathbf{i}}, \qquad (8)$$

where $\tilde{c}^{\dagger}_{\mathbf{i},\sigma}$ is the usual hole creation operator of the t-J model. $\hat{\phi}^{(n)}_{\alpha}$ is the symmetrized operator creating n phonons

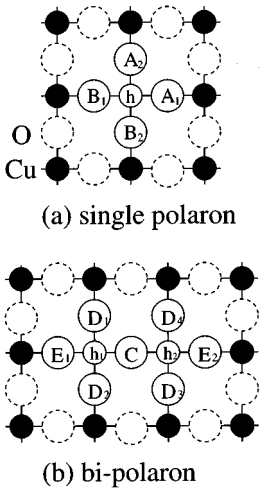

FIG. 8. Schematic oxygen sites for the phonon dressing to construct the single polaron (a) and bipolaron (b) operators. Those sites are labeled as A_1, A_2, B_1, ... h, h_1 and h_2 are the hole sites.

with the same local point-group symmetry as the one-hole ground state and Σ_α corresponds to the sum over all such independent n-phonon configurations. $[\cdots]_{\mathbf{i}}$ means that the boson part is centered around site $\mathbf{i}$. The coefficients $\gamma_\alpha^{(n)}$ (independent of $\mathbf{i}$) are determined so as to optimize the quasiparticle weight

$$Z_{1h}=\frac{|\langle\Psi_0^{N-1}|\overline{c_{\mathbf{k},\sigma}}|\Psi_0^N\rangle|^2}{\langle\Psi_0^N|\overline{c}^{\dagger}_{\mathbf{k},\sigma}\overline{c_{\mathbf{k},\sigma}}|\Psi_0^N\rangle}, \tag{9}$$

where Ψ_0^N and Ψ_0^{N-1} are the Néel and one-hole ground states, respectively, on the N-site cluster. We also define the operator $\overline{c_{\mathbf{k},\sigma,\alpha}^{(n)}}\equiv\Sigma_{\mathbf{i}}e^{i\mathbf{k}\cdot\mathbf{i}}\tilde{c}^{\dagger}_{\mathbf{i},\sigma}[\hat{\phi}_\alpha^{(n)}]_{\mathbf{i}}$. Since all the states $\overline{c_{\mathbf{k},\sigma,\alpha}^{(n)}}|\Psi_0^N\rangle$ are orthogonal to each other, the coeficients can be obtained as

$$\gamma_\alpha^{(n)}=\frac{\langle\Psi_0^{N-1}|\overline{c_{\mathbf{k},\sigma,\alpha}^{(n)}}|\Psi_0^N\rangle}{\langle\Psi_0^N|\overline{c_{\mathbf{k},\sigma,\alpha}^{(n)}}^{\dagger}\overline{c_{\mathbf{k},\sigma,\alpha}^{(n)}}|\Psi_0^N\rangle}. \tag{10}$$

The one-hole ground state of the $\sqrt{8}\times\sqrt{8}$ cluster has the momentum $\mathbf{k}=(\pi/2,\pi/2)$ and it is symmetric under the reflection with respect to $y=x$. Thus the independent sites for one-phonon dressing are A_1 and B_1 in Fig. 8(a). The two independent symmetrized one-phonon operators are written as $\phi_1^{(1)}=b_{A_1}^{\dagger}+b_{A_2}^{\dagger}$ and $\phi_2^{(1)}=b_{B_1}^{\dagger}+b_{B_2}^{\dagger}$. The four two-phonon operators can be given in the same way; $\phi_1^{(2)}=b_{A_1}^{\dagger}b_{A_2}^{\dagger}$, $\phi_2^{(2)}=b_{A_1}^{\dagger}b_{B_1}^{\dagger}+b_{A_2}^{\dagger}b_{B_2}^{\dagger}$, $\phi_3^{(2)}=b_{A_1}^{\dagger}b_{B_2}^{\dagger}+b_{A_2}^{\dagger}b_{B_1}^{\dagger}$, and $\phi_4^{(2)}=b_{B_1}^{\dagger}b_{B_2}^{\dagger}$. In the small coupling region, even restricting ourselves to dressed operators with up to one or two phonons is expected to provide a good description of the quasiparticle features.

The existence of a quasiparticle pole can be tested through the spectral function, which gives its dynamical properties. For the one-hole state, it is defined as

$$P_1(\omega)=\sum_l |\langle\Psi_l^{N-1}|\overline{c_{\mathbf{k},\sigma}}|\Psi_0^N\rangle|^2\delta(\omega-E_l^{(1)}+E_0^{(0)}). \tag{11}$$

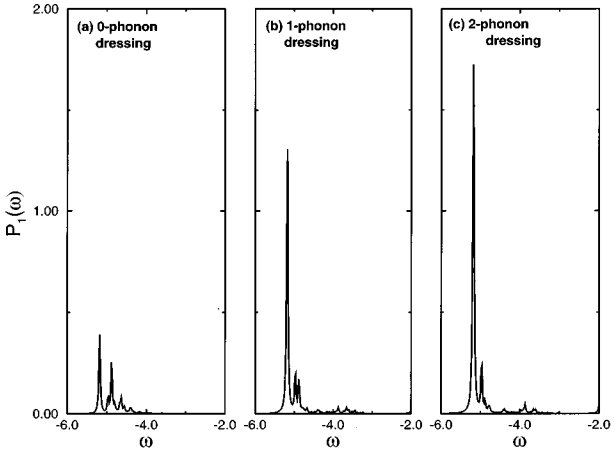

FIG. 9. Dynamical spectral function of a single polaron on Cu_8O_{16} with momentum $\mathbf{k}=(\pi/2,\pi/2)$ vs frequency in the presence of buckling modes for $J=0.4$, $\Omega=0.2$, and $\lambda_0=0.2$. Bare (a), one-phonon dressed (b) and two-phonon dressed (c) spectral functions have been considered.

It can be calculated by the standard technique based on the Lanczos algorithm. The spectral function of the quasiparticle at $\mathbf{k}=(\pi/2,\pi/2)$ for the buckling mode in the $\sqrt{8}\times\sqrt{8}$ cluster at $J=0.4$, $\Omega=0.2$, and $\lambda_0=0.2$ is shown in Fig. 9, where (a), (b), and (c) correspond to the results of the operator up to 0, 1, and 2 phonons taken into account, respectively. In our definition, the area of the peak at the bottom of the spectrum gives the quasiparticle weight with up to n-phonon dressing. Even for the bare operator, the quasiparticle can be distinguished and the peak becomes higher with increasing number of phonons, as shown in Fig. 9. Although the total area of the function changes with increasing dressed phonons, the peak at the bottom clearly grows up in comparison with higher-energy parts. Particularly, the gain of the peak due to dressing the first phonon is much larger than the second. It suggests that, for the present parameters used here, the dressed operator even up to one phonon can give a sufficiently accurate description of the quasiparticle.

B. Bipolaron

A bipolaron operator can be constructed in a similar way. We start from the conventional $d_{x^2-y^2}$ BCS spin singlet operator for nearest-neighbor sites $\hat{\Delta}_d=\Sigma_{\mathbf{i}}\Sigma_{l=0}^{3}(-1)^l[\hat{R}_{\pi/2}(\mathbf{i})]^l\{\tilde{c}^{\dagger}_{\mathbf{i},\uparrow}\tilde{c}^{\dagger}_{\mathbf{i}+\mathbf{x},\downarrow}\}$, where $\hat{R}_{\pi/2}(\mathbf{i})$ is the $\pi/2$-angle rotation of all the coordinates around the site $\mathbf{i}$. The bipolaron operator is given by

$$\overline{\Delta_d}=\sum_{\mathbf{i}}\sum_{l=0}^{3}(-1)^l[\hat{R}_{\pi/2}(\mathbf{i})]^l\left\{\tilde{c}^{\dagger}_{\mathbf{i},\uparrow}\tilde{c}^{\dagger}_{\mathbf{i}+\mathbf{x},\downarrow}\left[\Gamma^{(0)}+\sum_\alpha\Gamma_\alpha^{(1)}\hat{\Phi}_\alpha^{(1)}+\sum_\alpha\Gamma_\alpha^{(2)}\hat{\Phi}_\alpha^{(2)}+\cdots\right]_{\mathbf{i}}\right\}, \tag{12}$$

where each $\Phi_\alpha^{(n)}$ corresponds to an independent n-phonon creation operator. As previously, the coefficients $\Gamma_\alpha^{(n)}$ are determined by the optimization of the quasiparticle weight

$$Z_{2h}=\frac{|\langle\Psi_0^{N-2}|\overline{\Delta_d}|\Psi_0^N\rangle|^2}{\langle\Psi_0^N|\overline{\Delta_d^\dagger}\overline{\Delta_d}|\Psi_0^N\rangle}, \tag{13}$$

where Ψ_0^{N-2} is the two-hole ground state. Thus, each coefficient $\Gamma_\alpha^{(n)}$ can be obtained from a formula similar to Eq. (10). Independent one-phonon dressing operators for Δ_d are

$$\hat{\Phi}_1^{(1)}=b_C^\dagger,\quad \hat{\Phi}_2^{(1)}=b_{D_1}^\dagger+b_{D_2}^\dagger+b_{D_3}^\dagger+b_{D_4}^\dagger,$$

and

$$\hat{\Phi}_3^{(1)}=b_{E_1}^\dagger+b_{E_2}^\dagger,$$

where the points C, D_1, and E_1 are defined in Fig. 8(b). There are eight independent two-phonon dressing operators;

$$\hat{\Phi}_1^{(2)}=b_C^\dagger b_{D_1}^\dagger+b_C^\dagger b_{D_2}^\dagger+b_C^\dagger b_{D_3}^\dagger+b_C^\dagger b_{D_4}^\dagger,$$

$$\hat{\Phi}_2^{(2)}=b_C^\dagger b_{E_1}^\dagger+b_C^\dagger b_{E_2}^\dagger,$$

$$\hat{\Phi}_3^{(2)}=b_{D_1}^\dagger b_{E_1}^\dagger+b_{D_2}^\dagger b_{E_1}^\dagger+b_{D_3}^\dagger b_{E_2}^\dagger+b_{D_4}^\dagger b_{E_2}^\dagger,$$

$$\hat{\Phi}_4^{(2)}=b_{D_1}^\dagger b_{E_2}^\dagger+b_{D_3}^\dagger b_{E_1}^\dagger+b_{D_4}^\dagger b_{E_1}^\dagger+b_{D_2}^\dagger b_{E_2}^\dagger,$$

$$\hat{\Phi}_5^{(2)}=b_{D_1}^\dagger b_{D_2}^\dagger+b_{D_3}^\dagger b_{D_4}^\dagger,$$

$$\hat{\Phi}_6^{(2)}=b_{D_1}^\dagger b_{D_3}^\dagger+b_{D_2}^\dagger b_{D_4}^\dagger,$$

$$\hat{\Phi}_7^{(2)}=b_{D_1}^\dagger b_{D_4}^\dagger+b_{D_2}^\dagger b_{D_3}^\dagger,$$

and

$$\hat{\Phi}_8^{(2)}=b_{E_1}^\dagger b_{E_2}^\dagger.$$

The dynamical pair spectral function is defined as

$$P_2(\omega)=\sum_l |\langle\Psi_l^{N-2}|\overline{\Delta_d}|\Psi_0^N\rangle|^2\delta(\omega-E_l^{(2)}+E_0^{(0)}). \tag{14}$$

The function associated with the pair operator $\overline{\Delta_d}$ containing n-phonon dressing configurations where n is up to 0, 1, and 2, is shown in Figs. 10(a)–(c), respectively. When the bare operator is used as in Fig. 10(a), little spectral weight is seen at the bottom of the spectrum, in contrast to the pure t-J model.[12,13] Dressing the pair operator clearly changes drastically the low-energy features and a clear quasiparticle weight can be seen.

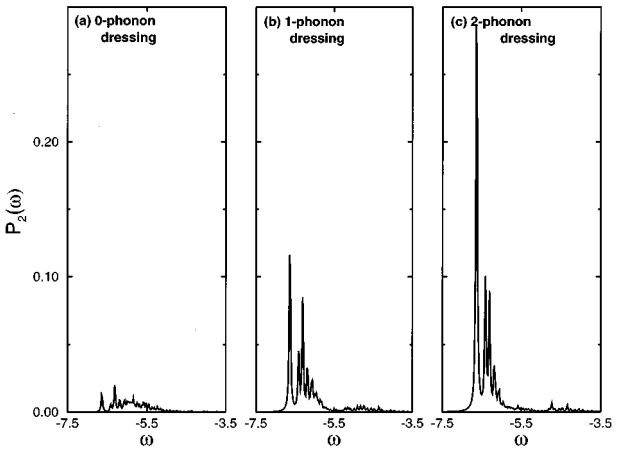

FIG. 10. Dynamical pair spectral function calculated on the Cu_8O_{16} cluster vs frequency in the presence of buckling modes for $J=0.4$, $\Omega=0.2$, and $\lambda_0=0.2$. Bare (a), one-phonon dressed (b) and two-phonon dressed (c) spectral functions have been considered.

VI. CONCLUSION

Exact diagonalization studies of the generalized 2D t-J-Holstein model give evidence for a stabilization of the two-hole pairing by out-of-plane buckling vibrations of the in-plane oxygens in the high-T_c cuprates. On the contrary, in-plane breathing modes suppress the pairing. The difference comes from the dynamical effect of the lattice displacements which cannot be reduced to a simple NN static interaction. We also found that the buckling mode does not give rise to any significant polaronic self-localization effect, in contrast to the breathing mode. In addition, we have constructed dressed pair operators which include dynamical phonon dressing and give large quasiparticle weights in the spectral function. Although photoemission experiments measure *a priori* the bare spectral function (and hence see rather small coherent features) it is not clear yet whether the dynamical features of the hole-lattice coupling described here could be tested experimentally.

ACKNOWLEDGMENTS

Laboratoire de Physique Quantique, Toulouse is Unité Mixte de Recherche du CNRS C5626. D.P. thanks J.R. Schrieffer and E. Dagotto for stimulating discussions. D.P. and D.J.S. acknowledge support from the EEC Human Capital and Mobility program under Grant No. CHRX-CT93-0332 and the National Science Foundation under Grant No. DMR95-27304, respectively. T.S. thanks the Yamada Science Foundation and SCC-ISSP for their support. We also thank IDRIS, Orsay (France), for allocation of CPU time on the C94 and C98 CRAY supercomputers.

[1] J. Zhong and H.-B. Schüttler, Phys. Rev. Lett. **69**, 1600 (1992).
[2] H. Röder, H. Fehske, and R. N. Silver, Europhys. Lett. **28**, 257 (1994).
[3] J. Frank, in *Physical Properties of High Temperature Superconductors IV*, edited by D.M. Ginsberg (World Scientific, Singapore, 1994).
[4] B. Normand, H. Kohno, and H. Fukuyama, Phys. Rev. B **53**, 856 (1996).

[5] J. Song and J. F. Annett, Phys. Rev. B **51**, 3840 (1995); **52**, 6930(E) (1995).
[6] N. Bulut and D. J. Scalapino, Phys. Rev. B **54**, 14 971 (1996).
[7] A. Nazarenko and E. Dagotto, Phys. Rev. B **53**, R2987 (1996).
[8] For derivations of low-energy effective electron-phonon Hamiltonians from three-band Hubbard models see, e.g., K. von Szczepanzki and K. Becker, Z. Phys. B **89**, 327 (1992).
[9] T. Holstein, Ann. Phys. **8**, 325 (1959).
[10] H. Fehske, H. Röder, and G. Wellein, Phys. Rev. B **51**, 16 582 (1995); G. Wellein, H. Röder, and H. Fehske, *ibid.* **53**, 9666 (1996), and references therein.
[11] D. Poilblanc *et al.*, Europhys. Lett. **34**, 367 (1996).
[12] E. Kaxiras and E. Manousakis, Phys. Rev. B **38**, 566 (1988); J. Bonča, P. Prelovšek, and I. Sega, *ibid*. **39**, 7074 (1989); J. Riera, *ibid*. **40**, 833 (1989); Y. Hasegawa and D. Poilblanc, *ibid*. **40**, 9035 (1989); D. Poilblanc, *ibid*. **48**, 3368 (1993).
[13] D. Poilblanc, Phys. Rev. B **49**, 1477 (1994); D. Poilblanc, J. Riera, and E. Dagotto, *ibid*. **49**, 12 318 (1994).
[14] In the pure t-J model, the average hole-hole distance is very sensitive to the parameter J/t as seen in Ref. 13.